Universitetet i Stavanger

FACULTY OF SCIENCE AND TECHNOLOGY

MASTER'S THESIS

Study programme/specialization: **Offshore Technology - Risk Management**	Autumn semester, 2017 **Open/~~Confidential~~**
Author: **Ji-eun Choi**	………………………………………… (signature of author)
Faculty Supervisor: **Jan Roar Bakke** External Supervisor: **Kees van Wingerden (Gexcon AS)**	
Title of master's thesis: **Application of FLACS to develop a standard for explosion venting of empty vessels**	
Credits: **30 ECTS**	
Keywords: Explosion venting, gas explosion, European standard, CFD modelling, FLACS	Pages: 42 pages + Appendix: 3 pages Stavanger, 12th December 2017

Abstract

Explosion venting is the most commonly used method to mitigate consequences of gas explosions. Therefore, research has been ongoing to establish adequate venting criteria for gas explosion. The existing standards are based on analytical models and empirical correlations. However, there are conflicts between the recommendations because of different factors influencing the peak overpressure that have been considered into such criteria or not.

Therefore, in this thesis work, a modified recommendation of venting criteria in gas explosion was proposed under assumption that one of the factors giving significant impact on overpressure was controlled. To obtain a wide range of data to support the proposed modification, various cases of vented gas explosions were simulated by using a CFD tool, FLACS. Furthermore, turbulence generation at equipment inside the enclosure and acoustic resonance were not taken into consideration to meet the assumption. Accordingly, FLACS which does not take into account the effect of acoustic resonance was used as the main tool to run the vented gas explosion simulations.

The proposed recommendation based on acquired results from FLACS simulations is less conservative than the existing recommendation suggested by Bradley & Mitcheson [1978], which has made reference to the aforementioned factors. Hence, it is expected that this work might help develop a guideline for explosion venting by proposing a modified safe recommendation in vent areas. However, the guideline shall specify that proper measures have to be implemented to eliminate the factors mentioned above.

Acknowledgment

I would like to express my deepest gratitude to my supervisors Kees van Wingerden and Jan Roar Bakke, who have guided me with valuable advice and encouragement. I would have not been able carry it out without your help.

Besides my supervisors, I would like to thank Gexcon AS for allowing me to write my thesis in collaboration with them and providing me their expertise, knowledge and resources.

I would also like to thank Camille, who instructed me how to use FLACS and helped me to settle down in the office.

My family in Korea and Gvarv for continued support and trust in me. Especially, Karen who has offered me a warm house, sincere friendship and mother-care during my stay in Bergen.

Also, my friends from the university, Albert, Minares and Turogalo who always give me warm advice and have made the last two years very special to me.

Lastly, my boyfriend, Fabian who has always been there for me with full support and love even when I was a little bit grumpy.

Table of Contents

List of Figures

List of Tables

Nomenclature

$\bar{A}$	Vent area ratio [-]
A_v	The vent cross section area [m^2]
A_s	The total area of the vessel, available for venting [m^2]
a_v	Speed of sound in the venting gas [m/s]
C_d	Coefficient of discharge for A_v [-]
$(dP/dt)_{max}$	Maximum rate of pressure rise [bar/s]
E_R	Equivalence ratio [-]
E	Combustion product expansion ratio [-]
K_G	Gas explosion constant [bar/s·m^{-1}]
P_a	Atmospheric pressure [bar]
$\bar{P}_c$	Cricital pressure ratio [-]
P_v	Venting pressure [bar]
P_{red}	Reduced explosion pressure [bar]
S_f	Flame speed [m/s]
S_u	Burning velocity [m/s]
S_v	Laminar burning velocity [m/s]
γ	Ratio of specific heats of the venting gas [-]
ρ_b	Density of burnt gas [kg/m^3]
ρ_{bv}	Density of burnt gas after constant pressure combustion at pressure P_v [kg/m^3]
ρ_u	Density of unburnt gas [kg/m^3]
ρ_{uv}	Density of unburnt gas at venting pressure P_v [kg/m^3]

Glossary

CASD   Computer Aided Simulation Design

CFD   Computational Fluid Dynamics

Ch   Chapter

Eq   Equation

EXP   Experiment

FLACS   Flame Accelerator Simulator

L/D   Length to Diameter relation

Porcalc   Porosity calculation

PROD   Combustion product mass fraction

SIM   Simulation

Blank page

1 Introduction

1.1 Background

Gas explosion is a frequently-observed accident in many industries. Therefore, there has been a lot of experimental research into the phenomena, and industry standards have been developed to limit the consequences of such accidental events.

There are several alternatives for mitigating gas explosions. And, explosion venting is the most commonly used method because of it being simple and cost effective (Bauwens & Dorofeev, 2013; Fakandu, Mbam, Andrews, & Phylaktou, 2016). Thus, considerable research devoted to the establishment of adequate venting criteria for explosions has been ongoing (van Wingerden & Zeeuwen, 1983a). Bradley & Mitchelson [1978] have suggested recommendation of safe vent area based on theoretical and experimental data. Solberg & Pappas [1981] and Van Wingerden [1983b] carried out experiments of vented gas explosion in large scale, and Harrison & Eyre [1987] studied external explosions as a result of explosion venting through a series of experiments in different size of vents and enclosure with several fuels.

When there is an explosion, the pressure increase during the early phases of the explosion pushes away the cover closing off the venting area in one of the walls of the protected enclosure (EN14994:2007). After the vent area is available, the pressure inside enclosure will increase less rapidly or will even decrease. This depends on the size of the vent opening and the combustion rate. The latter depends on several factors. Harrison & Eyre [1987] mention three important factors:

1) Turbulence inside the enclosure,
2) Combustion of gas outside the enclosure,
3) Acoustic resonances inside the enclosure.

Due to these factors influencing the combustion rate, the internal pressure does not always decrease after vent opening causing high-pressure peaks. However, knowledge of these factors affecting the combustion rate allows for influencing them and taking proper measures to reduce the maximum explosion pressure.

The existing engineering guidelines and standards such as EN 14994 [2007] have been made based on the analytical models and empirical correlations mentioned above, taking all or some of the factors mentioned above into account. However, the guidelines often have conflicting recommendations, due to the number of different factors that may influence the peak overpressure that have been taken into account or not (Helene H.Pedersen, 2012).

Several researchers argue that the occurrence of acoustic resonances during explosions inside vented enclosures in practice is seldom and can also easily be prevented from arising (Bauwens et al). Industry would therefore like to see a less conservative guideline being developed based on vented explosions in the absence of combustion affected by acoustic resonances.

The present thesis describes the work performed to develop such a guideline. The work focuses on the internal pressure in vented enclosures, with underlying assumption that

turbulence and acoustic resonances inside the enclosure have no impact on the internal pressure. Turbulence generation is only possible in the presence of obstructions inside the enclosure, hence the current work addresses empty enclosures only (i.e. enclosures without obstructions). Various volume of enclosures and vent area sizes will be tested by using FLACS software, which is the industry standard for CFD explosion modelling (Gexcon, 2017). The characteristic of FLACS not including the effect of acoustic resonances made it suitable for the assumption made in this work.

It is expected that this work may help developing a new standard for explosion venting which is less conservative than the existing one by getting rid of the two of the aforementioned influencing factors in internal pressure. The standard shall assure that elimination of the influencing factors is performed properly in practice.

1.2 Objectives
The detailed objectives of this study are as follows:

- A big variation of cases of vented gas explosions in empty vessels will be simulated by using FLACS.
- Based on the simulation results, a new safe recommendation will be proposed and compared to the one suggested by Bradley & Mitcheson [1978].

1.3 Scope of work
1) Modelling gas explosions for different conditions in vented enclosures using the CFD modelling tool FLACS, and analysing the internal pressures achieved.
2) Vented gas explosions will be simulated. The enclosures are near cubical with volume size 2 m^3, 4 m^3, 20 m^3 and 125 m^3. The vent sizes are chosen as a nominal fraction of the front wall area of the enclosures, which are $\frac{1}{16}, \frac{1}{8}, \frac{1}{4}, \frac{1}{2}, \frac{3}{4}$ and 1. Ignition location was normally chosen as central. Methane, ethylene, propane and hydrogen were used as fuels, and the fuel-air equivalence ratio was set to 1.1 for all the mixtures. Other than these main simulations, additional simulations were carried out varying parameters such as ignition source location, using two vents instead of one and different L/D ratio.
3) The two vent design standards, the European standard EN14994 [2007] and American standard NFPA68 [2013], use an approach based on the deflagration parameter $K_G = (dP/dt)_{max} V^{1/3}$ and the laminar burning velocity respectively. Both parameters were used in this work to observe different characteristics of the explosion process.
4) Suggestion of modifying vent safety equation by using data from FLACS simulations, and comparison with existing one derived by Bradley & Mitcheson [1978].

2 Methodology

2.1 Literature study

In order to study the mechanism of vented gas explosions and to obtain experimental data, several literature sources which report on research performed of the phenomena were consulted.

2.2 FLACS simulations

2.2.1 Introduction of FLACS

FLACS (Flame Acceleration Simulator) is a specialised computational fluid dynamics tool for safety applications developed by Gexcon AS. It can be used to study the consequences of the following process safety related processes:

- Dispersion of flammable or toxic gas
- Gas and dust explosions
- Propagation of blast and shock waves
- Pool and jet fires (FLACS Manual, 2017)

The software consists of three main parts, 1) Run manager, 2) CASD and 3) Flowvis.

1) Run manager

   Run manager is used to operate the FLACS simulator. It shows jobs that are ready to be simulated and you can choose which you want to start running. While simulation is going on, it plots time-pressure graph and log file.

2) CASD

   CASD is a pre-processor, abbreviation of Computer Aided Scenario Design. In CASD you can define scenarios, geometry and grid. Also, porosities of each grid can be calculated (see below for explanation).

3) Flowvis

   Flowvis is a post-processor. The results of simulations can be presented in 1D, 2D and 3D with variables that you set up as outputs during the pre-processor stage. (FLACS Manual, 2017)

The FLACS code uses a distributed porosity concept which enables the detailed representation of complex geometries (in some cases with up to 400.000 objects) using a Cartesian grid. Large objects and walls are represented on-grid, and smaller objects are represented sub-grid. This enables geometrical details to be characterized while maintaining reasonable simulation times. This approach represents geometrical details as porosities (opposite of blockage) for each control volume (Middha, 2010).

The FLACS manual presents detailed guidelines to set up geometry considering grid line etc. It has been found that one could get different results depending on grid size. This grid dependency has been studied in many papers, so it is not going to be discussed further in this

thesis. However, before setting up simulations, the grid sensitivity will be checked to find a suitable grid size for calculating reliable results.

2.2.2 Modelling and application limitations of FLACS in gas explosion

- It is important to represent the vent openings of a semi-confined geometry properly. If Porcalc adjusts the position of objects close to the outer boundaries to match the grid, the effective vent area may be affected. You should check the representation of the vent openings by verifying the porosity field in the post-processor Flowvis.
- FLACS does not simulate the effect of acoustic instabilities, which may dominate the explosion pressure for certain scenarios involving vented empty enclosures. However, obstructions, irregular surfaces and absorbing material (often present in real applications) will significantly decrease the importance of acoustic instabilities. Further details will be discussed later in this work (FLACS Manual, 2017).

3 Theory and definition

3.1 Gas explosion constant, K_G

K_G is maximum value of the pressure rise per unit time $(dp/dt)_{max}$ during the explosion of a specific explosive atmosphere in a closed vessel under specified test conditions normalized to a vessel volume of 1 m^3 multiplied by V$^{1/3}$ (EN14994:2007).

3.2 Laminar burning velocity and flame speed

A laminar combustion wave (reaction zone) propagates relative to the unburned gas of flammable mixture is the laminar burning velocity (Skjold et al.). This velocity is a fundamental property of the mixture and depends primarily upon the thermal diffusivity, chemical reaction rate, and heat of combustion (Kuchta, 1985).

The flame speed (S_f) is the velocity of propagation of the flame-front relative to the fixed point of ignition (Rallis & Garforth, 1980). Under adiabatic condition, the maximum S_f/S_u ratio is closer to approximately 7.5, which is typical of the combustion product expansion ratio (E) for most combustibles. Thus, the flame speed may be calculated from the flowing expressions (Kuchta, 1985):

$$S_f = S_u E \tag{1}$$

$$S_f = S_u \frac{\rho_u}{\rho_b} \tag{2}$$

S_f: Flame speed [m/s]

S_u: Burning velocity [m/s]

ρ_u: Density of unburnt gas [kg/m^3]

ρ_b: Density of burnt gas [kg/m^3]

3.3 Explosion venting

The European standard EN14994 [2007] states explosion venting as a protective measure preventing unacceptable high explosion pressure build-up inside enclosures. Weak areas in the walls of the enclosure open at an early stage of the explosion, releasing un-burnt gas/vapor and combustion products from the opening so reducing the overpressure inside the enclosure. Normally the explosion venting is applied such that the maximum reduced explosion pressure shall not exceed the known design pressure of the enclosure.
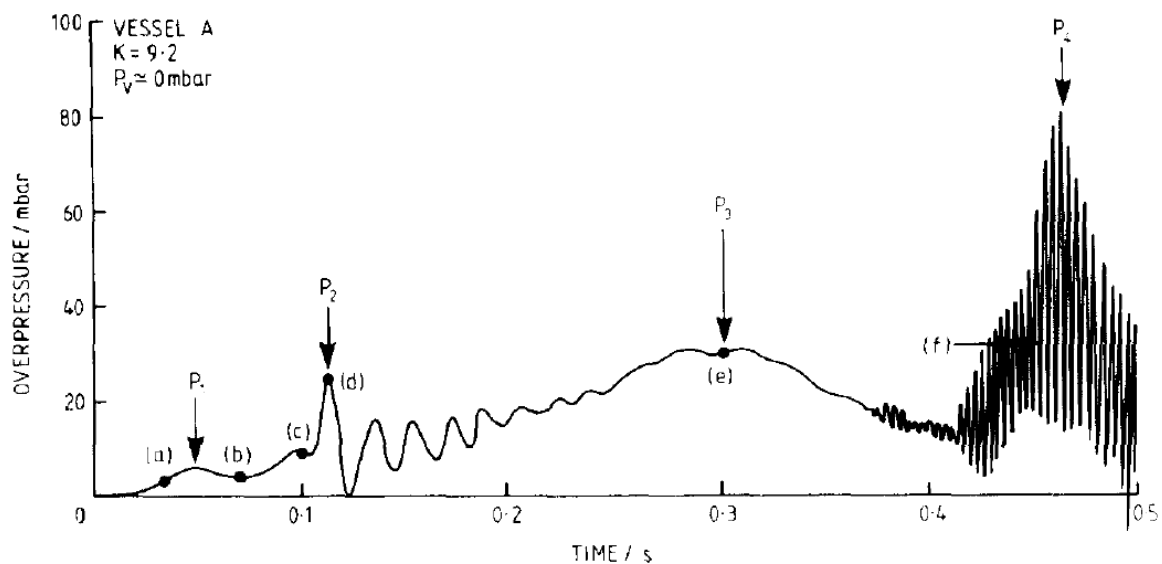
Figure 1. Pressure-time profile typical of an explosion in a near-cubic vessel with a low failure pressure explosion relief (Cooper, Fairweather, & Tite, 1986)

The pressure-time histories of explosions in compact vessels exhibit a multi-peak structure, with usually three peaks. The first peak (P_1) is a result of the vent starting to open, and has a value approximately equal to the vent burst pressure.

Following pressure relief due to venting, the second pressure peak occurs as a result of external combustion of unburned mixture expelled from the vessel. This peak was found to be important only in explosions involving low failure pressure relief panels or high burning velocity mixtures. The mechanism for the generation of this peak depends on the stage reached by combustion within the vessel at the time the flame front exits the enclosure. If combustion is at a sufficiently early stage that the burning rate within the vessel is relatively low, combustion outside the vessel influence the rising rate of internal pressure more than combustion inside the enclosure does. The reason is that the pressure wave generated by external explosion propagates back into the vessel, giving rise to P_2. On the other hand, if combustion burning rate inside the vessel exceeds that produced externally, P_2 will occur due to the reduction in the gas venting rate from the vessel (Cooper et al., 1986).

As the flame continues to expand it eventually encounters the walls of the vessel. At this point the rate of production of burned gas volume begins to decrease due to a reduction in flame area and the internal pressure starts to fall, giving rise to the third pressure peak P_3 (Cooper et al., 1986). P_4 is acoustically induced and was, in most cases, the largest peak of the four. This peak is capable of causing damage to enclosures if the venting arrangement does not take it

6

into account. In nearly all the tests reported by Lunn & Pritchard [2003] this large final peak was observed.

To apply explosion venting, the size of the vent and opening pressure of the vent cover have to be chosen so that the maximum internal pressure, the reduced explosion pressure (P_{red}), is below that which would cause failure of the enclosure. It may be acceptable to allow some damage to the enclosure, for example bowing of metal panels as deformation of expanded gas volume by explosion, provided this does not result in catastrophic failure of the vessel. Incorrectly sized relief vents will result in the plant not being properly protected (Lunn & Pritchard, 2003).

3.4 Simplified venting theory

Bradley & Mitcheson [1978] have introduced a simplified venting theory derived from basic equations of the rate of burning and the rate of venting. The relation used in the derivation is that the rate of venting should not be less than the rate of burning when the maximum rate of burning occurs (i.e., when the flame front is just touching the vessel walls). The equations obtained are as below.

$$\frac{\bar{A}}{\bar{S}} > \left(\frac{\gamma+1}{2}\right)^{\frac{1+\gamma}{2(\gamma-1)}} \qquad \text{for} \qquad P_a/P_v < \bar{P}_c \tag{3}$$

$$\frac{\bar{A}}{\bar{S}} > \left\{\frac{2}{\gamma-1}\left(\frac{P_a}{P_v}\right)^{\frac{2}{\gamma}}\left[1 - \left(\frac{P_a}{P_v}\right)^{\frac{\gamma-1}{\gamma}}\right]\right\}^{-0.5} \qquad \text{for} \qquad P_a/P_v > \bar{P}_c \tag{4}$$

$\bar{A}$: vent area ratio

γ : ratio of specific heats of the venting gas

P_a : atmospheric pressure [bar]

P_v : venting pressure [bar]

$\bar{P}_c$: cricital pressure ratio

In this simplification, important parameters were presented as following.

- Vent area ratio, $\bar{A}$

$$\bar{A} = C_d A_v / A_s \tag{5}$$

A_v: the vent cross section area [m^2]

C_d: Coefficient of discharge for A_v

A_s: the total area of the vessel, available for venting [m^2]

- Parameter, $\bar{S}$, is based on burning velocities and the speed of sound and is given by

$$\bar{S} = \frac{S_v}{a_v}\left(\frac{\rho_{uv}}{\rho_{bv}} - 1\right) \tag{6}$$

S_v: Laminar burning velocity [m/s]

a_v: Speed of sound in the venting gas [m/s]

ρ_{uv}: Density of unburnt gas at venting pressure P_v [kg/m^3]

ρ_{bv}: Density of burnt gas after constant pressure combustion at pressure P_v [kg/m^3]

Clearly, $\bar{S}$ is not a unique function of the initial mixture, but depends upon the value of P_v and the venting gas. Because of this, the parameter $\bar{S}_o$ was introduced which only depends on the initial mixture thus it is of greater utility, where

$$\bar{S}_0 = \frac{S_0}{a_{u0}}\left(\frac{\rho_{u0}}{\rho_{b0}} - 1\right) \tag{7}$$

S_0, ρ_{u0}, ρ_{b0} and other parameters with the suffix "0" are based on the initial conditions.

3.5   Factors influencing the internal pressure

In this chapter, factors influencing the internal pressure will be described, to obtain knowledge of these factors and to take proper measures to reduce influence of these factors.

3.5.1   Turbulence generated at obstructions

In a partly confined area with obstacles the flame may accelerate to several hundred meters per second during a gas explosion. The mechanisms causing the increased burning rate in turbulence deflagrations are the wrinkling of the flame front by large eddies and the turbulent transport of heat and mass at the reaction front. This turbulence is mainly caused by the interaction of the flow with structures and obstacles. Figure 2 shows how turbulence is generated when there are repeated obstacles in a channel. When the flame consumes the unburned gas, the products will expand. This expansion can be up to 8-9 times the initial volume. The unburned gas is therefore pushed ahead of the flame and a turbulent flow field may be generated. When the flame propagates into a turbulent flow field, the burning rate will increase dramatically. This increased burning rate will further increase the flow velocity and turbulence ahead of the flame (Bjerketvedt, Bakke, & van Wingerden, 1997).
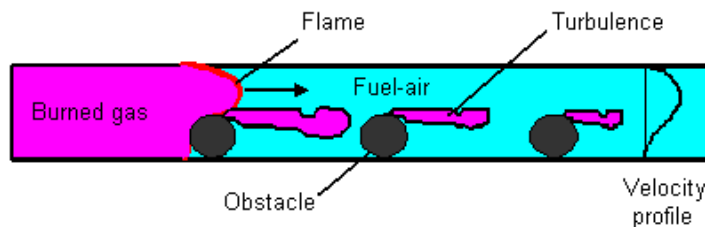
Figure 2. Turbulence generation in a channel due to repeated obstacles during a gas explosion
(Bjerketvedt et al., 1997)

3.5.2   Combustion of gas outside chamber

The internally generated pressures for large vent areas are low and the external peak overpressure gained is higher than the internal pressure. For small vent areas, the reverse is true. For this reason, the internal pressure of chambers with large vent areas can be influenced more by the external explosion. Also, explosions can occur at further distance depending on the size of vent areas. So, the effect of the external explosion is likely to be lower for small vent areas, because the size of pressure wave that can propagate into the chamber is smaller (Harrison & Eyre, 1987).
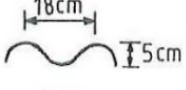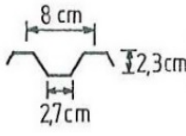
3.5.3   Acoustic resonances inside the enclosure

Acoustic resonance is a phenomenon where acoustic systems amplify sound waves whose frequency matches one of its own natural frequencies of vibration (Lawrence E. Kinsler, 1982) . Following the onset of these oscillations the rate of volume production by combustion increases sufficiently for the internal pressure to increase, the oscillations themselves being gradually damped out as the flame expands (Cooper et al., 1986).

In practice, rapid increase in gas velocity caused by a sudden opening of a vent produces a pressure wave. Such waves also may be generated by sudden changes in the rate of heat release. This occurs when the rate of change of flame area rapidly is reduced when the flame makes contact with the vessel wall. Such pressure and velocity disturbances may initiate a hydrodynamic instability within the flame front. This is turn, may be accompanied by an increase in the combustion rate and oscillatory pressure development (Mitcheson, 1978).

These acoustic waves appear as outstandingly high overpressure peak in pressure-time history. Van Wingerden & Zeeuwen [1983a] explain if the acoustic wave is eliminated, no third peak occurs, and carried out corresponding experiments. No other mechanism seems to be strong enough to generate a third peak. Experiments were performed in a vented 5.2 m^3 vessel to verify this. The tests were carried out by covering inner wall of a vessel with different damping materials and using propane-air mixtures only. The results are shown in table 1.

Table 1. Influence of lining the explosion vessel with damping materials on the pressure-time history of vented propane-air explosions in the 5.2m^3 vessel. Central ignition of quiescent mixture. vent area 1m^2. Static response pressure about 4.5 kPa (van Wingerden & Zeeuwen, 1983a).

Damping material	Lined vessel walls	propane concentration (%) v/v	amplitude (kPa)		
			1st peak	2nd peak	3rd peak
none	none	5,6	4,2	5,2	34,1
glass wool	sidewall + bottom	5,6	4,1	5,1	3,8
	2 sidewalls	5,5	4,1	5,7	3,1
	2 sidewalls + ceiling+bottom	5,3 / 6,0	3,6 / 4,0	5,8 / 3,4	0 / 0
corrugated plates (18cm, 5cm)	2 sidewalls + ceiling	5,2	1,9	5,8	0
(8 cm, 2,3cm, 2,7cm)	2 sidewalls + ceilings	5,4	2,6	1,2	0

As shown in table 1, the 3rd peak due to acoustic waves is negligible or disappeared in all of the cases tested after applying damping materials.

There are other parameters affecting acoustic flame instability. For example, installing obstacles in a vessel has been proved to impact this issue. It is likely that obstacles reduce the amplitude of this peak by disrupting acoustic waves in the chamber through the generation of multiple reflections and prevent acoustic coupling of the pressure waves to the flame surface (Bauwens & Dorofeev, 2013).

4 Gas explosion simulations by using FLACS

4.1 FLACS validation analysis through comparison of experiment and simulation

A comparison of experiment and simulation was carried out to confirm that FLACS is capable of predicting overpressures generated during vented gas explosions close to those seen in experiments. The validation concerns experiments described in an article of Harrison and Eyre [1987]. Figure 3 illustrates their experimental set-up. In the simulations, monitor points were mainly installed inside the chamber. An additional monitor point was installed outside, 5m away from the vent. This monitor point was included in the experiments to recognise external explosions and their possible influence on the explosions inside the enclosure. The tests were arranged in order (i.e. from B1 to B 18) in Harrison and Eyre [1987], and some of these tests were compared to simulation as shown in table 2.
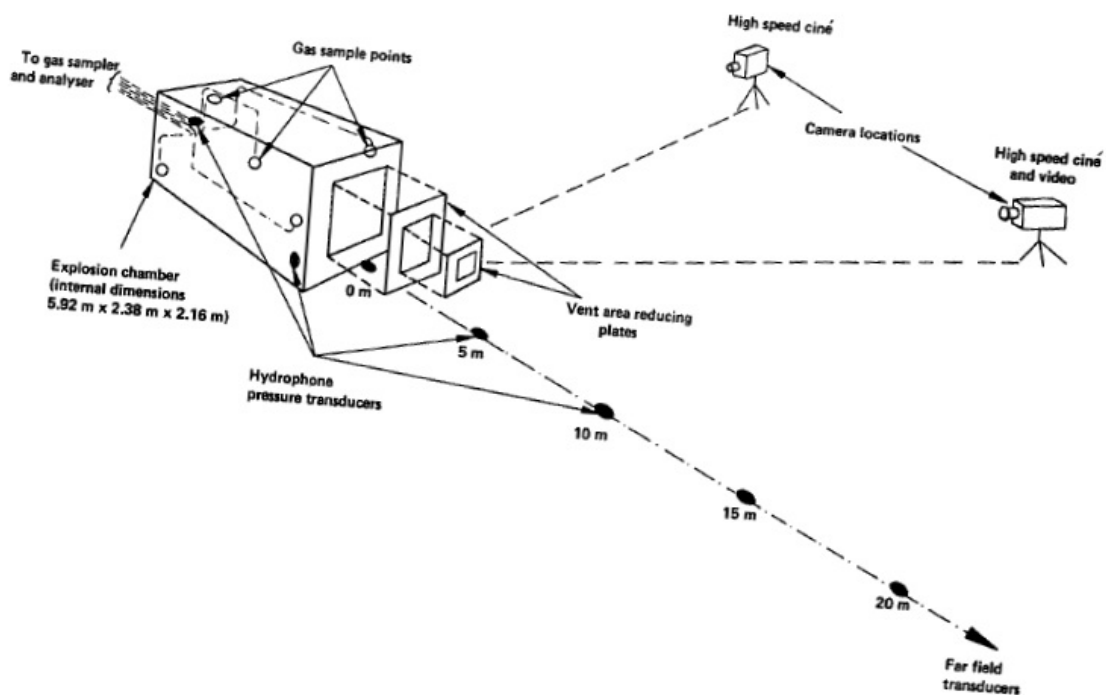

Figure 3. Schematic diagram of explosion chamber and instrumentation (Harrison & Eyre, 1987)

Table 2. Comparison of results from experiments and simulations

Test	Fuel	Vent[a]	Ignition location	ER	Peak overpressure at rear of chamber, *mbars*		Similarity index (exp/sim)	Peak overpressure recorded externally, 5m *mbars*		Similarity index (exp/sim)
					Exp	FLACS Sim.		Exp	FLACS Sim.	
B3	C_3H_8	1/2	Rear	1.10	286	271	0.95	227	201	0.89
B11	C_3H_8	1/4	Rear	1.11	1100	387	0.35	445	327	0.73
B18	C_3H_8	1/8	Rear	1.08	1340	1066	0.80	418	339	0.81
B5	N.G.	1/2	Rear	1.10	215	183	0.85	145	121	0.83
B7	N.G.	1/4	Rear	1.11	542	250	0.46	324	220	0.68
B16	N.G.	1/8	Rear	1.10	1067	1285	1.20	345	248	0.72

[a] *Nominal fractional areas of the front face*

The grid cell size used during the simulations was chosen to be 0.05 m according to recommendation from M.J. Klausen's [2016] work (Klausen, 2016). As can be seen in table 2, the results are in satisfactory agreement with experiments assuming a margin of error of ± 30 %. However, in the case of a vent size of ¼ of the front face, deviations are bigger.

The reason for the tests with the vent size ¼ are having much higher peak pressure in the experiments is explained by Harrison and Eyre [1987]. An external explosion due to the combustion of unburned gas pushed out of the vent can pose a far field blast hazard, but also inside the vessel the external explosion causes a pressure peak. In the far field the overpressure is determined both by overpressure peak at the source and the effective size of the pressure source. The peak pressure depends primarily on the vent flow rate, but the source size is dependent on the vent area. For example, for the smallest vent (1/8 area) the peak overpressure was higher due to a low vent flow rate, but the far field overpressure was lower than with the ¼ area vent due to the small source size. There is clearly an optimum condition for generation of the far field blast wave by an external explosion which maximises the product of the source size and peak overpressure. In the test conditions used by Harrison and Eyre [1987], this occurred with the ¼ area vent. There was insufficient data on which to base any general conclusion. However, it was noted that for very large vents the external explosion was weak and for very small vents the source size was small, thus the far field damage potential was minimal.

In the current investigation the interest was focused on internal pressure and the setup was not proper for observing external explosion and/or far field blast. There are different options that fit better to far field blast cases.

Also, FLACS has some limitations with regards to describing acoustic resonances inside a chamber. The acoustic pressure wave generated by the external explosion can propagate all the way through the vent into the chamber and give effect on internal pressure. For those situations where the internal pressure is significantly affected by the external overpressure, we would not expect normal vented explosion pressure prediction methods to apply, since they consider the internal combustion only (Harrison & Eyre, 1987).

4.2 Grid sensitivity analysis

To check grid sensitivity, gas explosion simulations in closed cubical boxes have been performed. The simulations were 3 different gases in 4 different volumes of enclosure with two grid sizes, which make a total 24 of setups. Suggested standard grid size is 0.1 m and the result of simulations using this grid size was compared to those obtained using different grid sizes.

As it was explained in Ch. 2.2, FLACS code uses calculation of porosity in each grid cell. Therefore, when there are significant differences in the number of cells per unit volume (1 m^3), one may obtain different results depending on the grid size. Hence, before using suggested standard grid size 0.1 m in different volumes of enclosures, grid sensitivity was checked. Simulations were run in two grid sizes, one was the standard grid size for all the volumes and the other was adjusted grid size which was almost linearly proportional to one line of an enclosure.

Table 3. Adjusted grid size depending on volume of enclosures

Volume [m^3]	Dimension [m]	Adjusted grid size, [m]	Number of cells in one line
2	1.3×1.3×1.2	0.025	52
4	1.6×1.6×1.6	0.04	40
20	2.7×2.7×2.7	0.05	54
125	5×5×5	0.1	50

The ignition point was set in the centre of the enclosure. The parameters chosen to assess the effect of grid size are the gas explosion constant, K_G and the flame speed. The reason why these two parameters are chosen, is that they contain information of fundamental properties of combustion reaction.

Figure 4 illustrates combustion product mass fraction changes in time. The measured points were ignition location and vent area. The flame speed was calculated by measuring the combustion product arrival time over the flame propagation distance from the ignition point to the vent area.
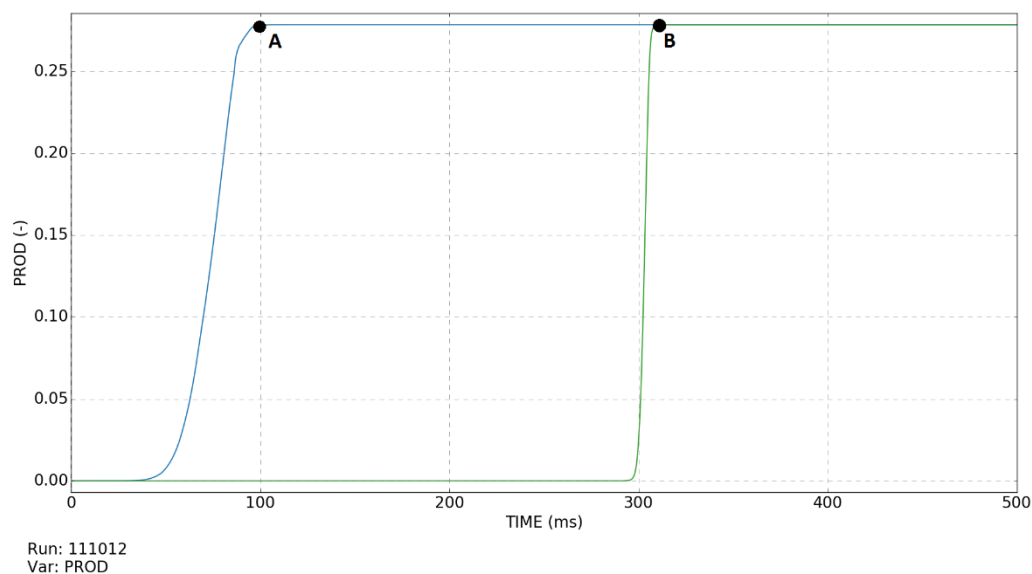

Run: 111012
Var: PROD

Figure 4. Combustion product mass fraction with regards to time from the ignition point to the vent area

13

In the paper of Lunn & Pritchard [2003], a modification of K_G is suggested because the K_G is vessel volume dependent. Therefore, they have analysed K_G in specific volumes and at specific pressure on pressure-time curve. K_{GV} is the K_G factor measured in cubical enclosed vessels of 2 m³, 4 m³ and 20m³, and $K_{GV(0.5)}$ is K_G measured at 0.5 bar g in the same enclosures used for K_{GV}. Table 4 shows gas explosion constant and flame speed obtained from the simulations of each fuel gas.

The average of the similarity columns of $K_{GV(0.5)}$, K_{GV} and flame speed are 1.13, 1.18 and 1.14 respectively. So, the margin of error in this comparison was 13% ~ 18% which is acceptable to continue further simulations using a grid size of 0.1 m.

Table 4. Comparison of K_{GV} and $K_{GV(0.5)}$ constants and flame speed in different grid sizes

METHANE	Volume m3	$K_{GV(0.5)}$ (bar/s)*m Sim			K_{GV} (bar/s)*m Sim			Flame Speed m/s Sim		
		Grid 0.1	Adj.Grid	Similarity	Grid 0.1	Adj.Grid	Similarity	Grid 0.1	Adj.Grid	Similarity
	2	23.94	23.94	1.00	81.89	54.18	1.51	6.40	6.55	0.98
	4	20.64	15.87	1.30	74.61	63.50	1.18	6.36	3.85	1.65
	20	19.00	19.54	0.97	73.29	62.43	1.17	6.26	4.79	1.31
	125	17.50	17.50	1.00	75.00	75.00	1.00	4.16	4.16	1.00

ETHYLENE	Volume m3	$K_{GV(0.5)}$ (bar/s)*m Sim			K_{GV} (bar/s)*m Sim			Flame Speed m/s Sim		
		Grid 0.1	Adj.Grid	Similarity	Grid 0.1	Adj.Grid	Similarity	Grid 0.1	Adj.Grid	Similarity
	2	52.92	42.84	1.24	270.88	194.03	1.40	11.43	11.17	1.02
	4	47.62	34.92	1.36	261.92	215.89	1.21	10.85	7.94	1.37
	20	43.43	38.00	1.14	249.73	238.87	1.05	9.57	9.71	0.99
	125	45.00	45.00	1.00	275.00	275.00	1.00	9.72	9.72	1.00

PROPANE	Volume m3	$K_{GV(0.5)}$ (bar/s)*m Sim			K_{GV} (bar/s)*m Sim			Flame Speed m/s Sim		
		Grid 0.1	Adj.Grid	Similarity	Grid 0.1	Adj.Grid	Similarity	Grid 0.1	Adj.Grid	Similarity
	2	35.28	32.76	1.08	166.31	117.17	1.42	7.90	8.00	0.99
	4	33.34	25.40	1.31	158.74	133.34	1.19	7.48	5.50	1.36
	20	29.86	27.14	1.10	157.44	146.58	1.07	6.80	6.91	0.98
	125	32.50	32.50	1.00	175.00	175.00	1.00	7.11	7.11	1.00

5 Discussion of vented gas explosion with different comparison standards

The following work is focused on the internal pressure in vented enclosures, under the assumptions that turbulence and acoustic resonances inside the enclosure have no impact on the internal pressure.

5.1 Brief description of simulation set-ups

In this chapter, the simulations of vented gas explosions will be discussed. The conditions of the simulations of vented gas explosions used are presented below.

a) Gas type: methane, ethylene, propane and hydrogen
b) Mixture concentration: the simulations were always performed for an equivalence ratio of 1.10 for each of the gases
c) Ignition point: the centre of the enclosures
d) Volume of the enclosures: 2 m^3, 4 m^3, 20 m^3 and 125 m^3
e) Shape: the enclosures had an L/D=1. The enclosures were effectively cubical.
f) Pressure panel: pressure relief panel was installed on one front face of the enclosures. One requirement of an effective explosion relief panel is that it should possess as low a failure pressure as possible in order to ensure pressure relief of the protected vessel at an early stage in the explosion process (Cooper et al., 1986). Detailed settings are shown below in table 5.
g) Initial conditions: no turbulence, temperature 20 C° and ambient pressure 10^5 Pa.

Table 5. Pressure relief panel setting in simulations

Position	Center of one front face
Size	$\frac{1}{16}, \frac{1}{8}, \frac{1}{4}, \frac{1}{2}, \frac{3}{4}$ and 1 of front face
Type	Pop out
Opening pressure	0.1 bar g
Weight	1.0 kg/m^2

h) Monitor points: The monitor points are located in the centre of the rear wall, the centre of the vent area, the centre of the box, and 5m outside from vent area.
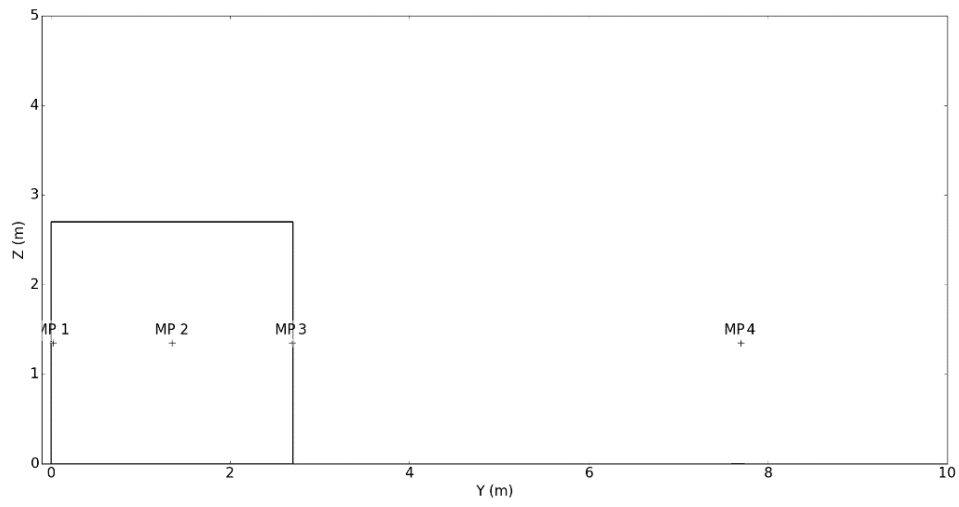i) Initial conditions: no turbulence, temperature 20 C° and ambient pressure 10^5 Pa.

Figure 5. Schematic diagram of an enclosure used in simulation with monitor points

Figure 6. Simulation 3D plot, central ignition and 125 m^3 of an enclosure with pressure relief panel
(1/2 of the front wall area)

16

5.2   Volume of the enclosures

Figure 7 shows a comparison of internal pressure-time histories obtained in different sizes of enclosures. The pressure was measured at a monitor point in the centre of the rear of the box. The volumes of the enclosures were 2 m^3, 4 m^3, 20 m^3 and 125 m^3. Gas type was propane with equivalence ratio 1.10, and vent area is 1/8 of front wall for all 4 cases. The pressure relief panel has opening pressure of 0.1 bar which was early enough of combustion process.
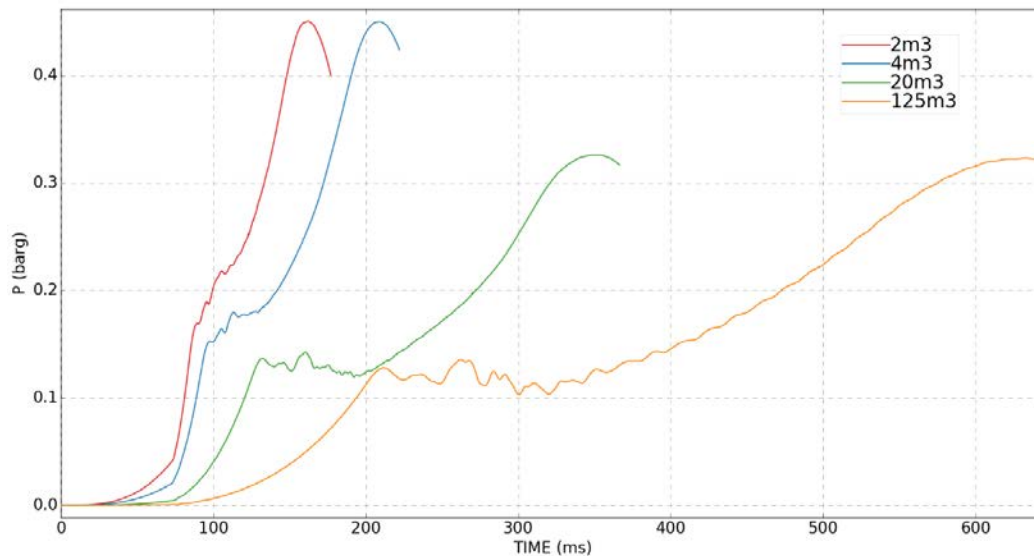
Figure 7. Internal pressure-time history of vented explosion with propane in 4 different volumes of enclosures. Vent size is 1/8 of front face

With central ignition, prior to failure of the relief panel, the flame front expands roughly spherically from the ignition point. The flame surface is mainly smooth during this combustion phase. Once the pressure inside the vessel, generated by the production of burned gas volume, exceeds the relief failure pressure, the relief panel begins to move away from the vent, allowing unburned fuel-air mixture to escape from the enclosure (Cooper et al., 1986).

There is no standing out pressure peak after venting due to the relatively small size of the vent area. Instead, internal pressure keeps increasing as the combustion rate (rate of generation of combustion products) is higher than the volumetric flow rate of unburned gas out of the vent. The pressure starts decreasing when there is more gas expelled through the vent than combustion gas generated inside.

As it is illustrated in figure 8, it takes more time to fail the vent panel in the bigger volumes of vessels since it has more fuel to burn to reach the opening pressure, 0.1 bar. And that results in lower maximum pressure in bigger volumes, because in these volumes there is time to establish sufficient flow of unburned gas out of the vent (Cooper et al., 1986).

5.3 Vent area size

Internal pressures for different vent area sizes are compared in figure 8 below. The size of chamber was 4 m^3 (1.6 m×1.6 m×1.6 m) filled with propane 4.41 % (volume percentage). Five different vent area sizes were taken into consideration: $\frac{1}{16}, \frac{1}{8}, \frac{1}{4}, \frac{1}{2}$ and 1 of front face. The pressure was monitored in the centre of the enclosure coinciding with the location of the ignition point.

The vent opening pressure was 0.1 bar. For the cases of vent area size ¼, ½, and 1, as opening of the vent unburned gas flows out, the internal pressure started falling and making the 1st pressure peak appearing clearly. The first pressure peak is also maximum internal pressure for these cases since the vent area is large enough to expel unburned gas from the chamber to outside. During the combustion process, unburned gas keeps flowing out and it distorts the flame from its original spherical shape, extending it to the vent. When the distorted flame front reaches the vent opening, burnt gas with low density discharged from the chamber. The volumetric flow of the gas rises because of the decrease of the density of vented gas. This results in drop off the internal pressure, as volumetric flow of the gas eventually exceeds the volume production by combustion (Cooper et al., 1986). This mechanism appears as 2nd peak for the cases with a vent size ¼ and above in figure 8.
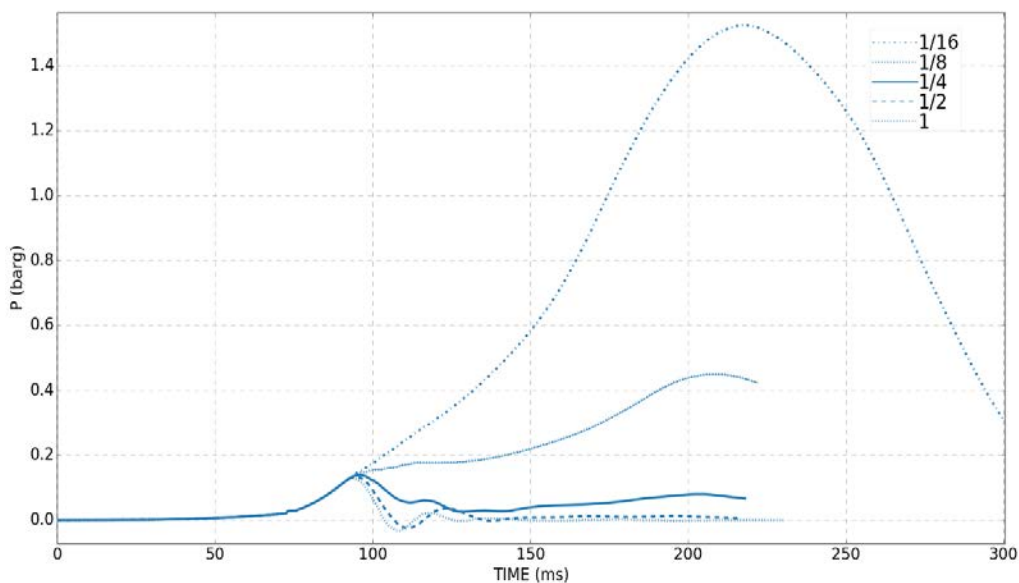

Figure 8. Comparison of the effect of vent size in a vented enclosure of 4 m^3 with Propane 4.41%

On the other hand, ones with smaller vent area size: 1/8 and 1/16, do not show a pressure peak right after vent opening. As the flame grows, its surface area expands, and then the rate of volume production by combustion exceeds the volumetric flow rate through the vent, and the internal pressure keeps on increasing. The smaller the size of the vent the higher the internal pressure as shown in figure 9, since the volumetric flow rate out of the vent will be lower accordingly.
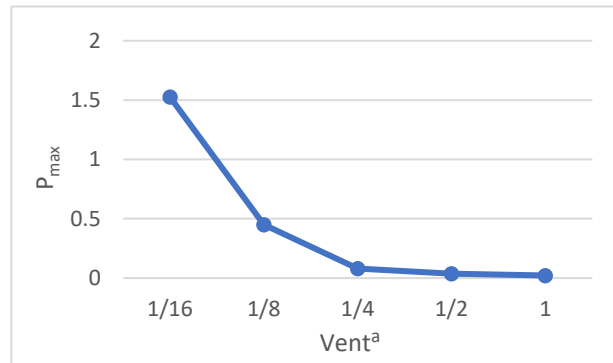
Figure 9. Relation between vent size and maximum internal pressure
ᵃNominal fractional areas of the front face

5.4 Different gas types

In this chapter, the effect of using different gas types will be discussed. Hydrocarbon gases; ethylene, propane and methane were chosen for the comparison. These different combustible gases mentioned above have different chemical and physical characteristics (burning velocity), which influence the internal pressure build-up.

The laminar flame speed is the measured rate of expansion of the flame front in a combustion reaction under laminar flow conditions (Taylor, 1991).

The laminar flame speed of three fuel-air mixtures determined experimentally is presented in table 6. For hydrocarbon-air mixtures one may say that the higher the laminar flame speed, the more reactive is the mixture. This means that the flame can propagate fast through a cloud and thereby cause flame acceleration and pressure build-up (Bjerketvedt et al., 1997).

Table 6. Laminar flame speed for Stoichiometric composition (Bjerketvedt et al., 1997)

	Ethylene	Propane	Methane
S (m/s)	6.5	4	3.5

Figure 10 shows FLACS simulation results. It shows internal pressure measured in the centre of the enclosures of 4 m^3 with vent size ¼ of the front face. The maximum overpressure in all cases is slightly above the vent opening pressure, 0.1 bar with slight differences, as 0.155 bar, 0.132 bar and 0.117 bar for ethylene, propane and methane respectively. However, the mixture with higher flame speed reaches higher pressure in the shorter time, reflecting the effect of the inertia of the vent panel.
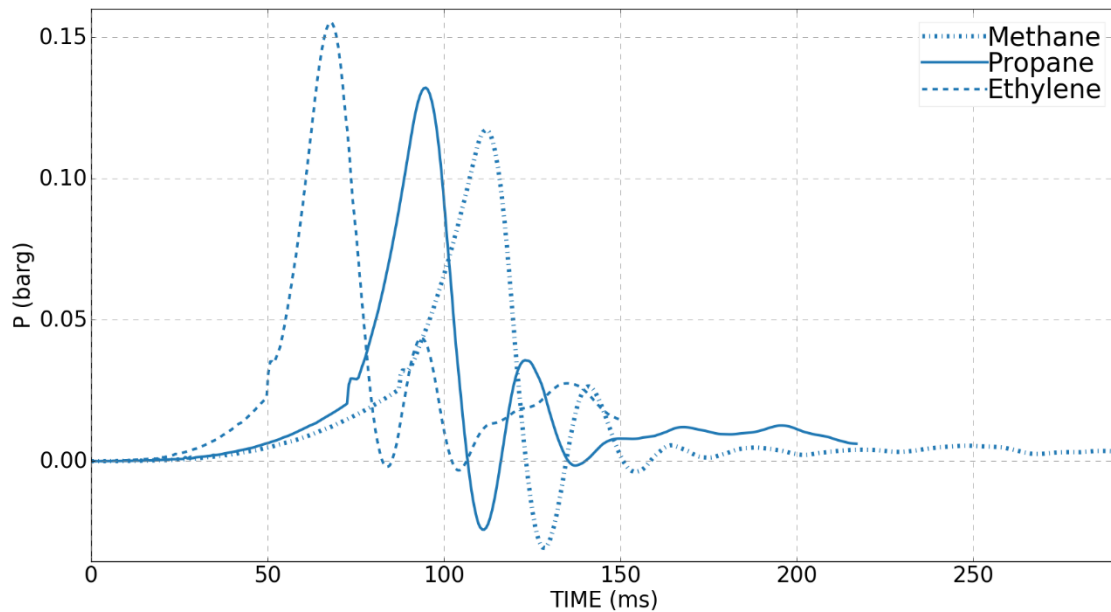
Figure 10. Pressure-time history in different fuel-air mixtures, measured in the center of the enclosures of 4m^3 with vent area size ¼ of the front face

5.5 Additional variations

Additional simulations with some variations have been performed to investigate how the maximum internal pressure changes in different conditions. The chosen variations are adjusting ignition location, installing two vents instead of one vent, and elongation of near cubical enclosures. To limit the number of simulation cases, fuel gas was defined to be propane, volume of enclosures was set to 4m^3, and 5 vent sizes: $\frac{1}{16}, \frac{1}{8}, \frac{1}{4}, \frac{1}{2}$ and 1 of front face were investigated.

5.5.1 Ignition source location

Three different ignition source locations were designated, one in the centre of the rear wall (later referred to as rear wall ignition), another in the centre of the enclosure (centre ignition) and the other in the centre of the vent area (front wall ignition). Figure 11 presents change of internal pressure with regards to time.

As it is shown in figure 11, the maximum internal pressure in the cubical box with centre ignition reaches higher value compared to either rear ignition or vent area ignition. In the case of centre ignition in a cubical box, the flame surface is exposed more to combustible gas than the other two cases. Also, unburned gas in the back corners is located in difficult

position to be expelled through the vent, since the flame in the centre expands in all directions in a sphere shape.

For the rear ignition case, as the flame expands it contacts the walls resulting in a smaller flame surface area than seen for centrally ignited flames. On the other hand, turbulence is generated at the walls increasing the combustion rate.

By igniting near the vent opening the combustion products will be vented almost immediately and the flow velocity and the turbulence in the unburned mixture will be low (Bjerketvedt et al., 1997). Burnt gas flows out right away and unburned gas inside the chamber will be burned slowly. As one can see in figure 11, each curve ends up when there is no more fuel. It takes more than 400 ms to burn all the fuel in the case of vent area ignition, whereas centre ignition case finishes burning the fuel in 300 ms and the rear ignition consumes the fuel in less than 250 ms.
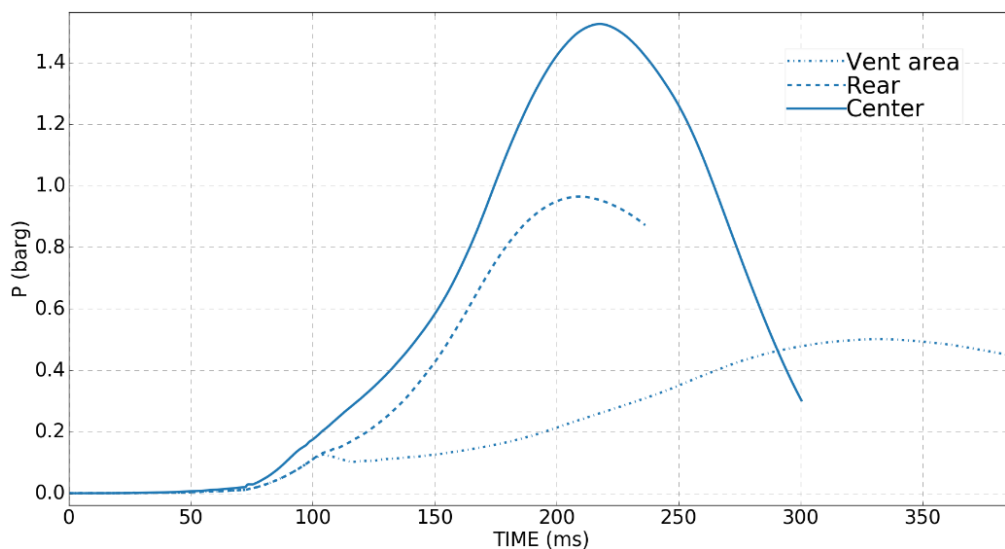
Figure 11. Pressure-time history depending on different ignition source locations in 4m^3 of near cubical enclosures with vent area size 1/16 of the front face

5.5.2   Two vents instead of one vent

So far all discussed vented explosions were with one vent on the front-end wall of the enclosures. In this chapter vented explosions having two vents will be discussed compared to one vent explosion. The total size of vent area was equal regardless of the number of vents. In case of one vent explosion, the vent panel was installed on the front wall and its size was 1/8 of the front face. In case of two vents explosion, the vent panels were installed on the front and the back walls and each vent size was 1/16 of one end face.

Even though nearly same condition was applied for the two cases described above, there was a difference in maximum internal pressure of almost 0.1 bar by dividing vent area into two and installing one of them on the other side in line with same axis.

The pressure-time history in these two cases are illustrated in figure 13. The slope of two graphs are decreasing after reaching the vent opening pressure, 0.1 bar. The vent size was not big enough to drop the internal pressure immediately. Therefore, the internal pressure keeps

21

increasing slowly again after the venting. The rates of pressure increase in both conditions are very similar still. Figure 12 shows a cross-section of when the products of combustion flow out through the vent. The difference between the two explosions is clearly happening towards the end of the combustion. In case of one vent a lot of combustion occurs in the part of the volume far away from the vent. The venting in this case is less effective than when there two vents and the distance between areas where combustion still takes place and the vent opening is relatively short.

Figure 14 shows a comparison of two cases with different numbers of vent opening, where the total vent size was ½ of the front face. Compared to figure 13, these two graphs in figure 14 have similar movement. The 1st peaks in both cases are around 0.13 bar and the 2nd peaks of them are around 0.04 bar, also the rest parts of the graphs are quite close as well. It means that when the vent is big enough to allow a high volumetric flow rate through the vent than volume production by combustion, the number of vents does not matter as long as the total vent area size is the same.
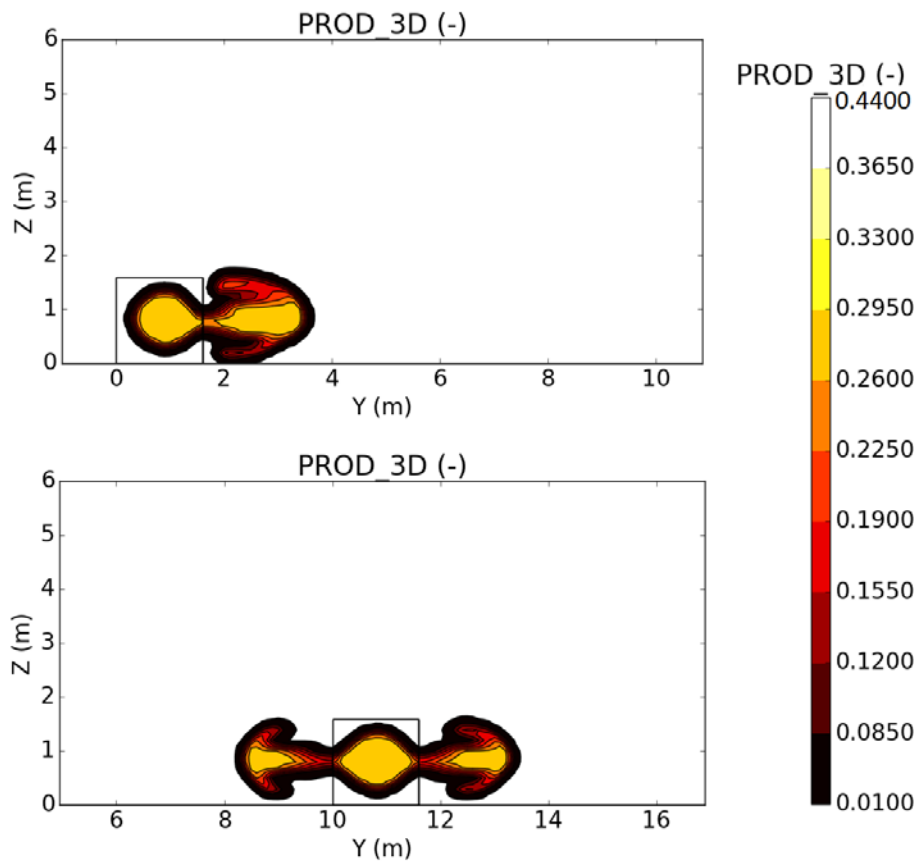
Figure 12. 2D cut plane of 4 m^3 chambers with pure propane-air mixture with ER 1.1. One vent explosion (top) and two vents explosion (bottom)
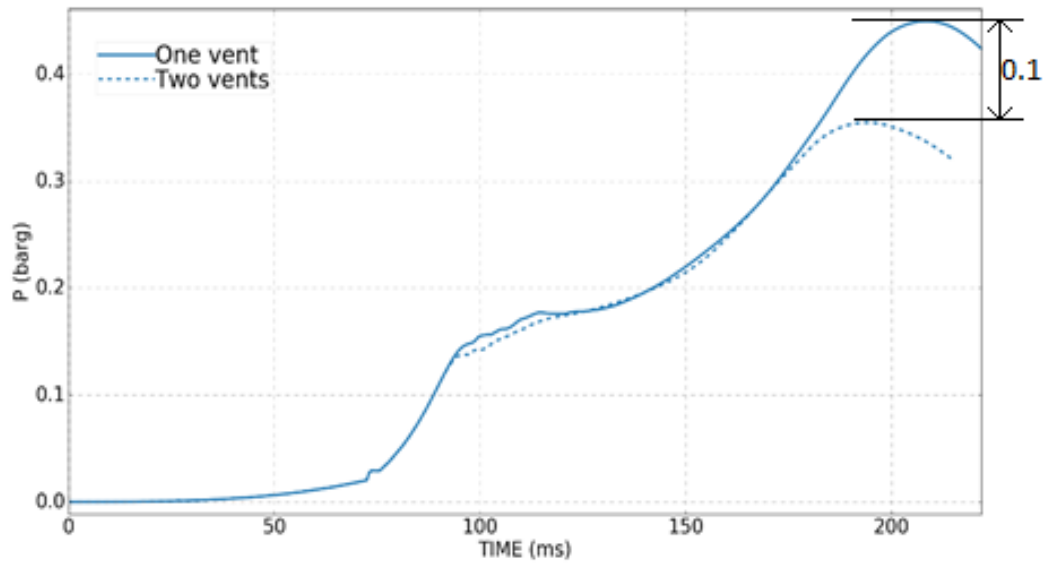
Figure 13. Pressure-time history of 4 m^3 of enclosures with different numbers of vent opening, total vent size: 1/8 of the front face in both cases
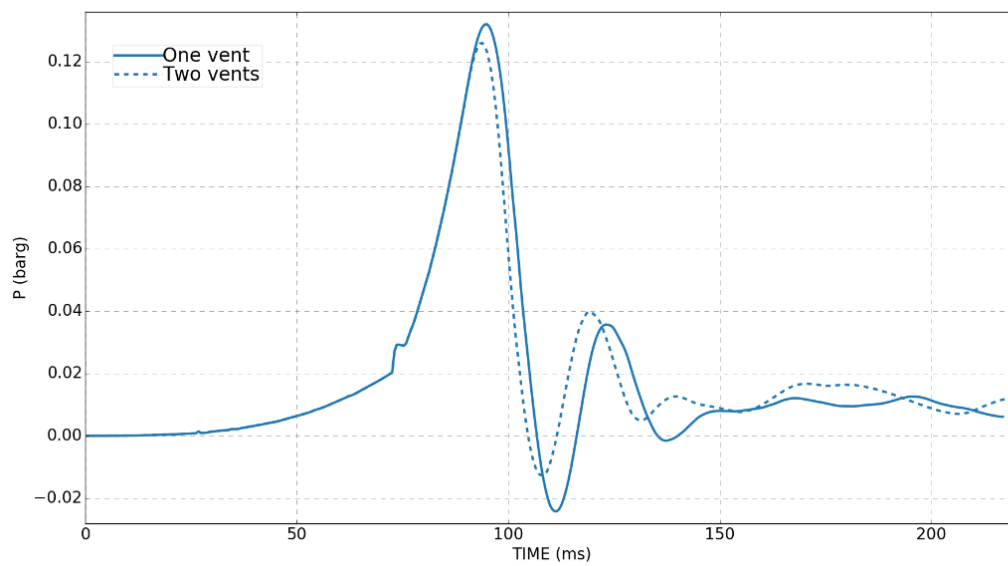

Figure 14. Pressure-time history of 4 m^3 of enclosures with different numbers of vent opening, total vent size: 1/2 of the front face in both cases

5.5.3 Variation of L/D

The last variation taken into consideration is variation of L/D. L/D ratio 1, 2 and 4 were applied as shown in figure 15. All the other initial conditions besides L/D ratio were controlled to be same. The total volumes of enclosures were maintained around 4m^3 and the vent panel size was 0.3 m^2(0.6 m×0.5 m) in all L/D ratio. Detailed dimensions of the enclosures are specified in table 7. The used fuel was pure propane mixed with air to equivalence ratio 1.1. And it was ignited on the centre of the back wall.

Table 7. Detailed information of enclosure dimensions depending on L/D ratio

L/D Ratio	Dimension (x, y, z) [m]	Volume [m^3]	Vent size [m^2]
1	1.6×1.6×1.6	4.096	0.3
2	1.1×3.2×1.1	3.872	0.3
4	0.8×6.4×0.8	4.096	0.3

Figure 16 shows pressure-time history in these three enclosures. The pressure was measured in the centre of each enclosure. In all cases, it does not give outstanding pressure drop off by vent opening because the vent area size was not sufficient. But the maximum internal pressure shows differences. It is expected to see higher maximum pressure as L/D ratio increases.

If venting of combustion products is not sufficient to keep the flame speed at a low level, flame propagation distance is the stronger factor than the venting to influence internal pressure. By increasing the distance of the flame propagation, the flame can be accelerated rapidly while traveling the longer distance which will result in high pressure (Bjerketvedt et al., 1997). Accordingly, the case with the highest elongation ratio shows significantly higher maximum pressure peak compared to the other two cases.

However, the two cases with L/D=1 and L/D=2 do not have significantly different maximum internal pressure. In some period, the one with L/D=1 is showing even slightly higher pressure than the other (L/D=2). This might be explained with the acceleration of the flame. The accelerated flame speed caused by having enough distance to develop the speed makes the flow rate of burnt gas through the vent increase. Even though the differences in maximum pressure peak is not great, still the elongated one reaches higher pressure than cubical enclosure.

And the effect will be even greater if there are obstacles to pass by. This effect will be most pronounced when one or more of the following apply: very reactive fuel, high density of obstructions, small vent areas or large obstructed volumes (Bjerketvedt et al., 1997).
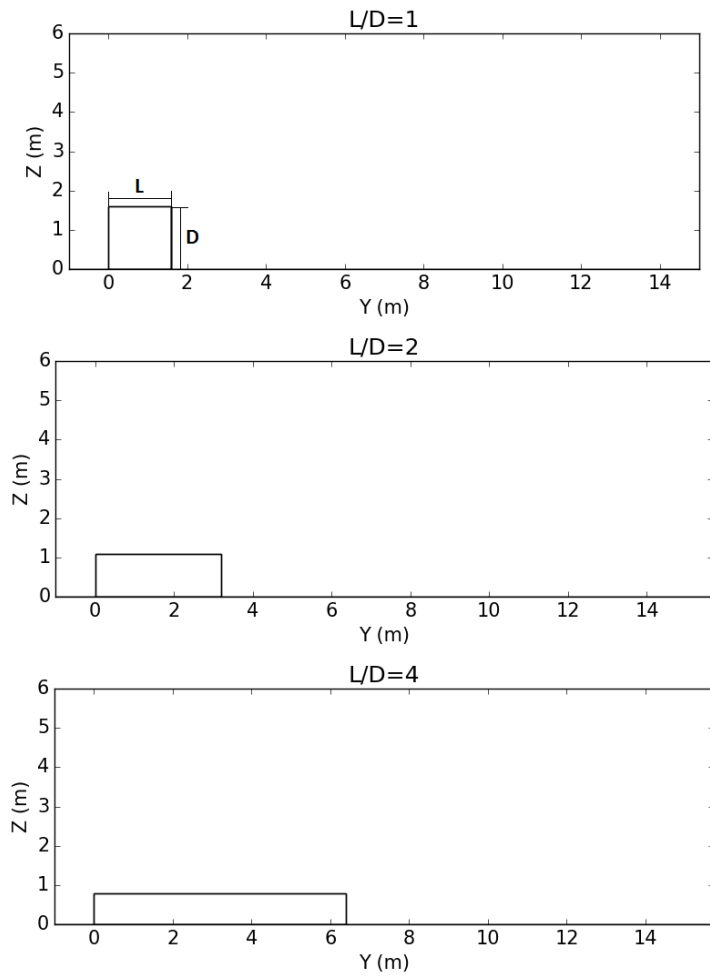
Figure 15. 2D cut plane of different L/D ratio enclosures
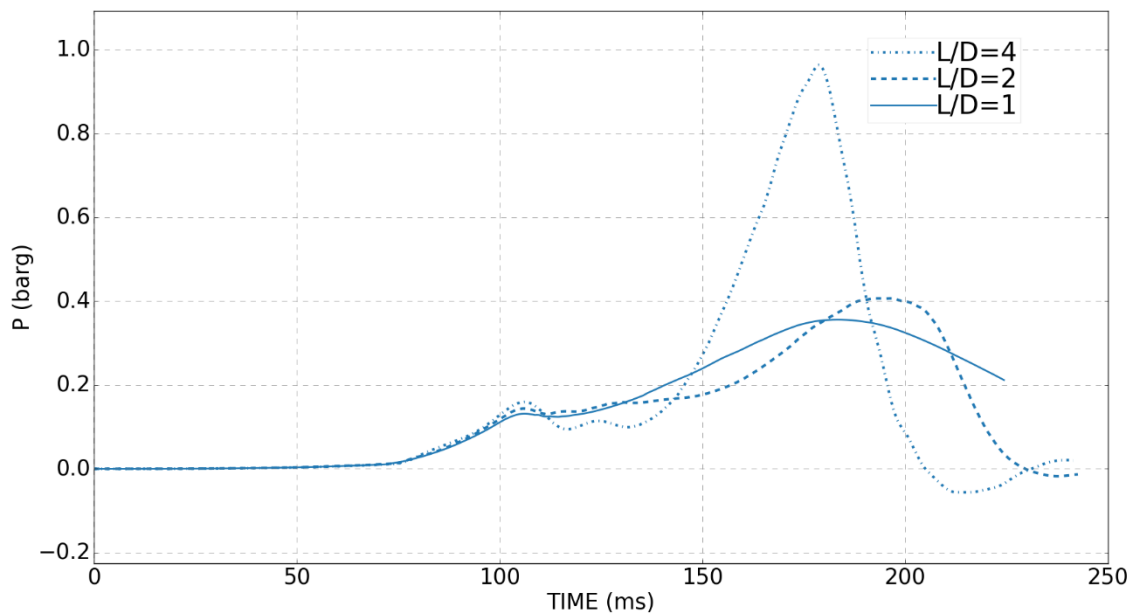
Figure 16. Pressure-time history depending on L/D ratio

6 Evaluation of results and proposal for venting equation

Bradley & Mitcheson [1978] suggested the safe recommendation for covered vent areas as shown in Figure 17 based on their theoritical model and experiments. Recommendations for the selection of safe vent areas are proposed in terms of parameter $\bar{A}/\bar{S}_0$ for central ignition of initially quiescent pre-mixed gases in near spherical or cubical containers. It is presented as the variation of maximum pressure rise, ΔP_m atmospheres, above atmospheric for different values of $\bar{A}/\bar{S}_0$.
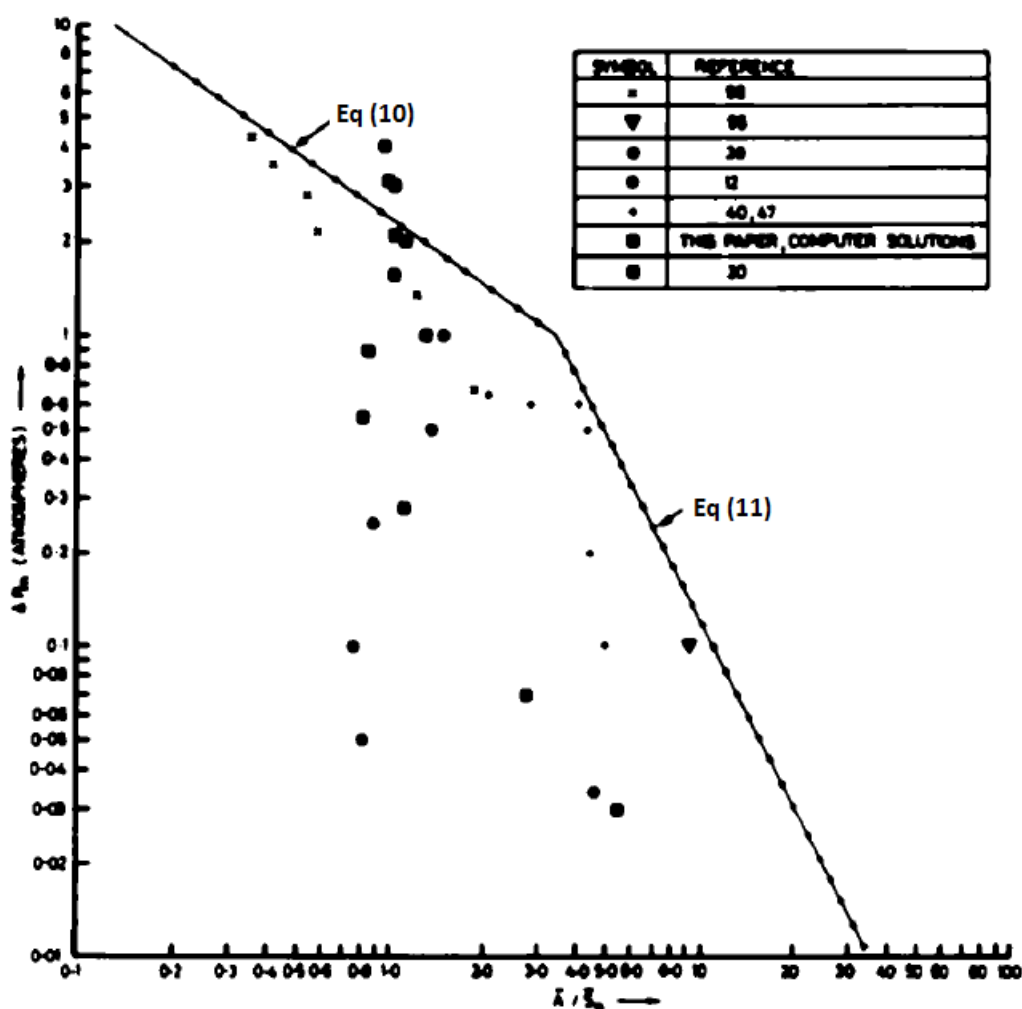
Figure 17. Safe recommendations for covered vent areas (Bradley, 1978)

In most cases it has been assumed that the vents behave as sharp-edged orifices, with a value of C_d equal to 0.6. The present procedure is to indicate values of $\bar{A}/\bar{S}_0$ at which the second pressure peak (i.e. maximum pressure after opening of the vent) is equal to P_v. For higher values of $\bar{A}/\bar{S}_0$ the second pressure peak is less than P_v. Asterisked values from these figures are shown in figure 17 and the full line dotted curve has been constructed to enclose them. This is given by two equations (Bradley, 1978).

$$\frac{\bar{A}}{\bar{S}_0} > \left(\frac{2.4}{P_v - 1}\right)^{1.43} \tag{8}$$

for $P_v > 2$ atmospheres

$$\frac{\bar{A}}{\bar{S}_0} > \left(\frac{12.3}{P_v - 1}\right)^{0.5} \tag{9}$$

for $P_v < 2$ atmospheres, and arrange equation (8) and (9) with regards to P_v, then they become

$$P_m = P_v = 1 + 2.4(\bar{A}/\bar{S}_0)^{-0.7} \tag{10}$$

for $\Delta P_m > 1$ atmosphere and,

$$P_m = P_v = 1 + 12.32(\bar{A}/\bar{S}_0)^{-2} \tag{11}$$

for $\Delta P_m < 1$ atmosphere.

To compare the previously obtained results from simulations to the suggested safe recommendation, the results are plotted in the recommendation graph as shown in figure 18.

Figure 18. Safe recommendation of Bradley & Mitcheson [1978] combined with results from FLACS simulations

27

The ΔP_m values were chosen from pressure-time history graph in each case. When vent size was big enough to generate 1st pressure peak caused by vent opening, the pressure in all cases is close to the vent opening pressure. Accordingly, 2nd pressure peak was chosen to be plotted in. As decreasing the vent size it had less effect on the first peak relative to the effect on the second one, due to the interplay of various factors (Bauwens, Chaffee, & Dorofeev, 2010). Thus, the first peak was often shown as small fluctuations and the graph reached the maximum pressure as more fuel is burned. Eventually, in all vent sizes the maximum pressure after vent opening was chosen to be recorded in the graph.
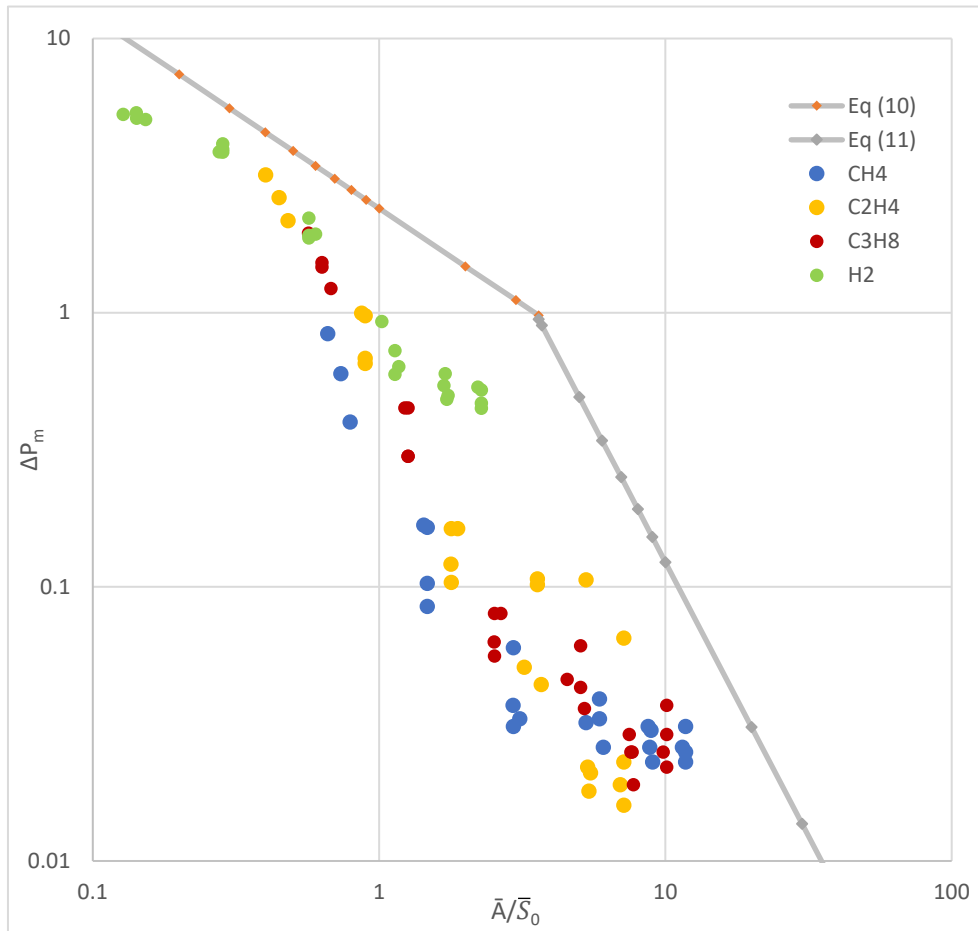
All the results from FLACS simulations were plotted and compared to the safe recommendation. To check how well experiments are fitted into the recommendation, some results from works by Bauwens [2013] and Skjold.T et al., [2017] have been taken as comparison. Experiments of Bauwens [2013] were applied with different gas composition and back wall ignition, and used propane gas. Experiments of Skjold.T et al., [2017] were varied with vent size, used hydrogen gas and had central ignition. Both cases were without obstacles. Oscillatory combustion was not seen in these experiments. Detailed information about the experiments are presented in table 8.

Simulations with the exact same condition of these experiments have been conducted to ensure that the results from FLACS simulations are showing similar behaviour. All the results are illustrated in figure 19. The experiments and simulations show rather similar behaviour to each other, however the maximum pressures from both experiments and simulations are much lower than the safe recommendation at the same value of $\bar{A}/\bar{S}_0$.

Table 8. Set-up of the experiments by Bauwens [2013] and Skjold.T et al., [2017]

	Gas	Volume $[m^3]$	$\bar{S}_0$	Gas composition		Vent area			
				Vol.%	ER	A $[m^2]$	$\bar{A}$	$\bar{A}/\bar{S}_0$	Location
Bauwens [2013]	Propane	64	0.0099	4.8	1.2	5.4	0.033224	3.3560	Front wall
		64	0.0099	5.2	1.3	5.4	0.033224	3.3560	Front wall
		64	0.0099	5.6	1.4	5.4	0.033224	3.3560	Front wall
Skjold [2017]	Hydrogen	33	0.044	21	0.7	4	0.035797	0.8136	On the top
		33	0.044	21	0.7	6	0.053695	1.2203	On the top
		33	0.044	21	0.7	8	0.071594	1.6271	On the top
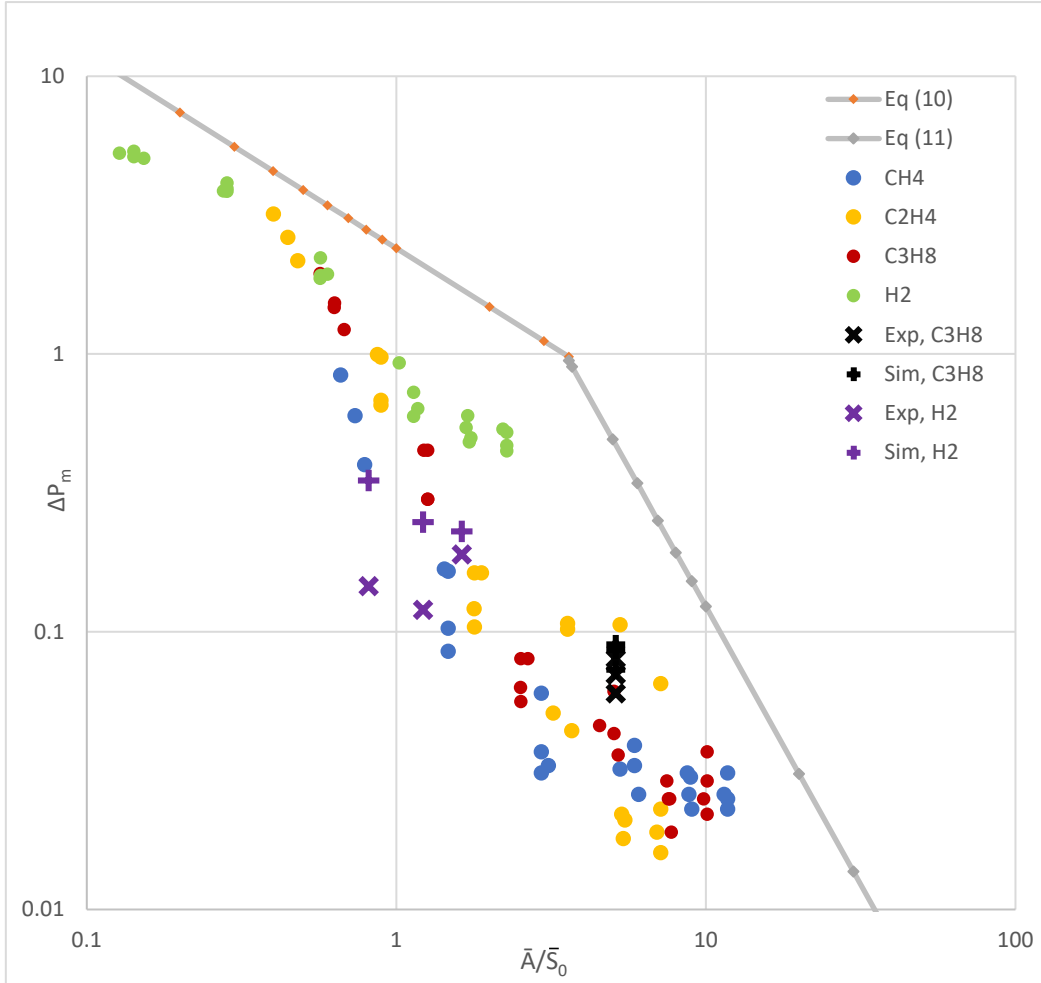
Figure 19. Safe recommendation of Bradley & Mitcheson [1978] combined with results from FLACS simulations and experiments from Bauwens [2013] & Skjold.T et al., [2017]

On the basis of the series of results from simulations and experiments discussed, a modification of equations (10) and (11) is proposed as following.

$$P_m = P_v = 1 + 1.8(\bar{A}/\bar{S}_0)^{-0.65} \tag{12}$$

for $\Delta P_m > 1$ atmosphere and,

$$P_m = P_v = 1 + 7.5(\bar{A}/\bar{S}_0)^{-2.2} \tag{13}$$

for $\Delta P_m < 1$ atmosphere.

By applying the modified equations, ΔP_m values with regards to $\bar{A}/\bar{S}_0$ have been reduced. Considering that the existing recommendation has made reference to the role of oscillatory combustion during venting, the proposed equation should have lower ΔP_m values than the existing one as presented in figure 20.

Furthermore, the results from the additional simulations assessing various additional factors (section 5.5) were indicated in figure 20 to check if the variations can be enclosed in proposed graph. Safety margin was not necessary to consider in this case, since all the extreme cases were plotted and enclosed in the proposal.
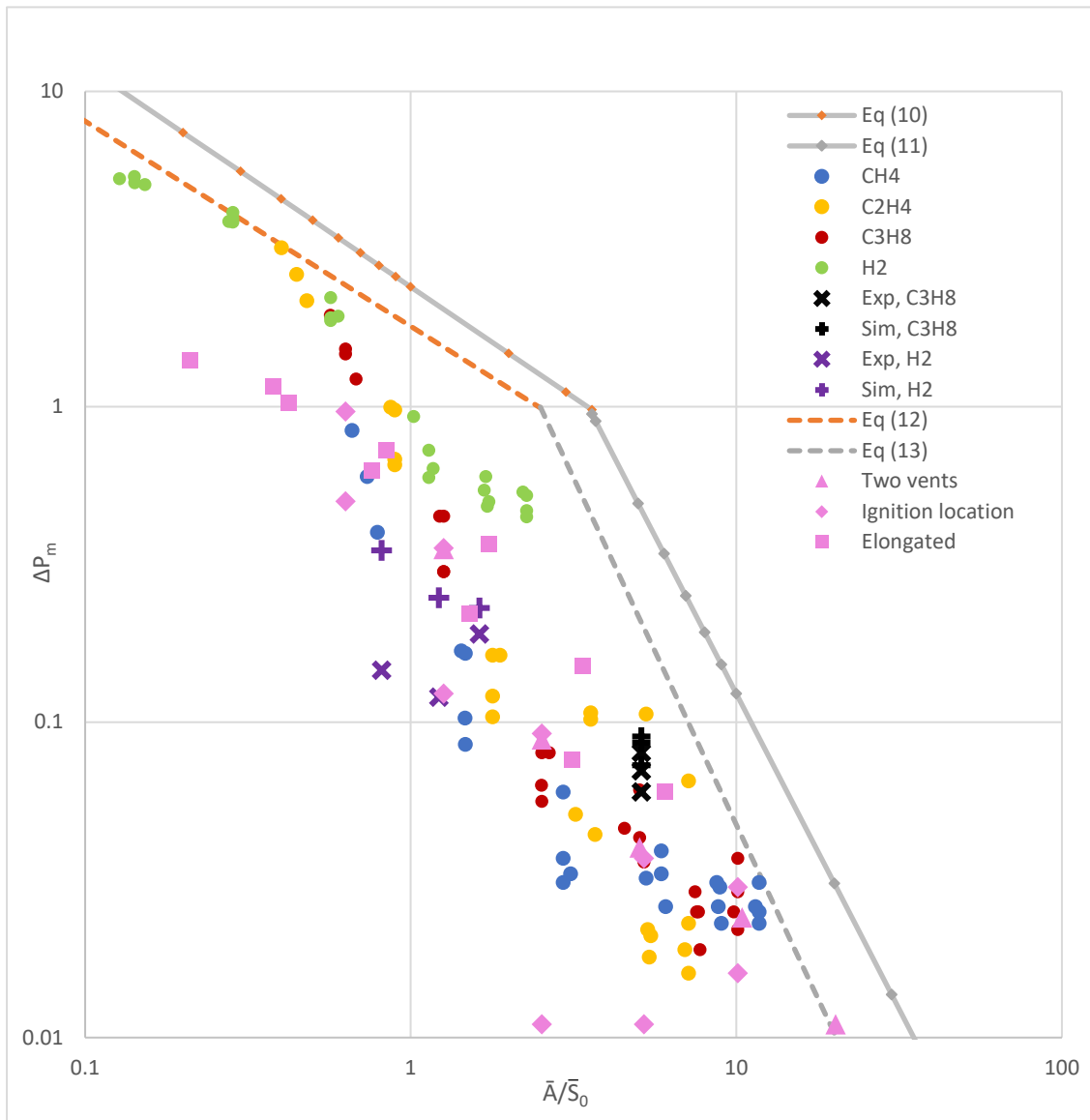
Figure 20. Proposed safe recommendation compared to Bradley & Mitcheson's [1978] suggestion.

7   Conclusion

Vented gas explosions in empty vessel have been simulated by using FLACS. The simulation results discussed in this thesis work were maximum internal pressure after vent opening, and the results have been discussed with different comparison standards such as volumes of enclosures, vent area sizes and different gas types.

When the vented gas explosion simulations in different volumes of enclosures were carried out, it was seen that the maximum internal pressure decreased as the volume of the enclosure increased. The reason is that in the cases of bigger volumes there is enough time to establish sufficient flow of unburned gas out of the vent. With comparison standard of vent sizes, it showed results as expected. The maximum internal pressure stayed around the vent opening pressure when the vent size was sufficient, but it increased as the vent size got smaller. When it comes to different gas types, the maximum internal pressure was higher when the reactivity of the gas was greater. A gas with high reactivity has faster flame speed which causes higher internal pressure, and it will require larger vent size to mitigate consequences when there is gas explosion.

Additional variation has been also reviewed to obtain wide range of results. The first variation was ignition location, which was varied as back wall ignition, centre ignition and front wall ignition. The centre ignition reached higher internal pressure compared to the other two conditions, since the flame surface was exposed more to combustible gas. Next variation was setting up two vents instead of one vent. Total vent area size was controlled to be the same, but in case of two vents, the vent panels were installed on both front and back wall. When the vent size was small, the case with two vents worked more efficiently than the other case with one vent. However, when the vent size was big enough, both cases showed similar behaviour in pressure-time graph. The last variation was differences in L/D ratio. With greater L/D ratio, the maximum internal pressure increased, because the flame gets accelerated by travelling longer distance and that results in high pressure build up.

All of the simulation results in different conditions were plotted and compared to the safe recommendation for covered vent areas of Bradley & Mitcheson [1978]. Based on the simulation results, a modified safe recommendation was proposed in this thesis. As presented in figure 20, the proposed safe recommendation has lower maximum internal pressure, because the role of oscillatory combustion was not taken into consideration.

The current work has been carried out with the underlying assumptions that turbulence and acoustic resonances inside the enclosure do not influence the internal pressure. The reason is that only empty enclosures were considered, and the effect of acoustic resonances can be removed by taking proper measures. These assumptions made using of FLACS software advantageously, since it does not reflect the effect of acoustic resonance. It is expected that this work might help developing less conservative guideline for explosion venting by proposing modified safe recommendation in vent areas. However, the guideline shall specify that proper measures are implemented to eliminate the factors mentioned above.

References

1) Bauwens, C. R., Chaffee, J., & Dorofeev, S. (2010). Effect of ignition location, vent size, and obstacles on vented explosion overpressures in propane-air mixtures. *Combustion Science and Technology, 182*(11-12), 1915-1932.
2) Bauwens, C. R., & Dorofeev, S. B. (2013). Parameters Affecting Flame-Acoustic Flame Instabilities in Vented Explosions.
3) Bjerketvedt, D., Bakke, J. R., & Van Wingerden, K. (1997). Gas explosion handbook. *Journal of hazardous materials, 52*(1), 1-150.
4) Bradley, D. a. A. M. (1978). The Venting of Gaseous Explosions in spherical Vessels. II - Theory and Experiment. *COMBUSTION AND FLAME, 32*, 237-255.
5) Cooper, M., Fairweather, M., & Tite, J. (1986). On the mechanisms of pressure generation in vented explosions. *COMBUSTION AND FLAME, 65*(1), 1-14.
6) Gas explosion venting protective systems (EN14994:2007).
7) Gexcon, Webpate. (2017). Retrieved from http://www.gexcon.com/
8) Fakandu, B. M., Mbam, C. J., Andrews, G. E., & Phylaktou, H. N. (2016). Gas Explosion Venting: External Explosion Turbulent Flame Speeds that Control the Overpressure. *CHEMICAL ENGINEERING, 53*.
9) Harrison, A., & Eyre, J. (1987). External explosions" as a result of explosion venting. *Combustion Science and Technology, 52*(1-3), 91-106.
10) Helene H.Pedersen, P. M. (2012). Modelling of Vented Gas Explosions in the CFD tool FLACS. *CHEMICAL ENGINEERING TRANSACTIONS, 26*. doi:10.3303/CET1226060
11) Klausen, M.-J. (2016). *Vented gas and dust explosions-External explosions.* The University of Bergen,
12) Kuchta, J. M. (1985). *Investigation of fire and explosion accidents in the chemical, mining, and fuel-related industries: a manual*: US Department of the Interior, Bureau of Mines.
13) Lawrence E. Kinsler, A. R. F., Alan B. Coppens, James V. Sanders (Ed.) (1982). *Fundamentals of Acoustics* (3rd Edition ed.): Wiley.
14) Lunn, G., & Pritchard, D. (2003). *A modification to the K~ G method for estimating gas and vapour explosion venting requirements.* Paper presented at the INSTITUTION OF CHEMICAL ENGINEERS SYMPOSIUM SERIES.
15) FLACS Manual, F. v. U. (2017). FLACS v10.6 User Manual. In (10.6 ed.): Gexcon AS.
16) Middha, P. (2010). Development, use, and validation of the CFD tool FLACS for hydrogen safety studies.
17) Mitchelson, D. B. a. A. (1978). The Venting of Gaseous Explosions in Spherical Vessels. I - Theory. In (Vol. 32, pp. 221-236): COMBUSTION AND FLAME.
18) NFPA68. (2013). Standard on Explosion Protection by Dflagration Venting. In: National Fire Protection Association (NFPA).
19) Rallis, C. J., & Garforth, A. M. (1980). The determination of laminar burning velocity. *Progress in Energy and Combustion Science, 6*(4), 303-329.

20) Skjold, T., Hisken, H., Lakshmipathy, S., Atanga, G., van Wingerden, M., Olsen, K. L., . . . Van Wingerden, K. (2017). *Influence of Congestion on Vented Hydrogen Deflagrations in 20-foot ISO Containers: Homogeneous Fuel-Air Mixtures.* Paper presented at the ICDERS.

21) Solberg, D., Pappas, J., & Skramstad, E. (1981). *Observations of flame instabilities in large scale vented gas explosions.* Paper presented at the Symposium (International) on Combustion.

22) Taylor, S. C. (1991). *Burning velocity and the influence of flame stretch.* University of Leeds,

23) Van Wingerden, C., & Zeeuwen, J. (1983a). On the role of acoustically driven flame instabilities in vented gas explosions and their elimination. *COMBUSTION AND FLAME, 51*, 109-111.

24) Van Wingerden, C., & Zeeuwen, J. (1983b). *Venting of gas explosions in large rooms.* Paper presented at the 4th Int'l Symp. on Loss Prevention and Safety Promotion in the Process Industries, EFCE Publication Series.

Appendix A

Appendix A contains detailed information of simulations and experiments data used in Chapter 6.

Table 9. Detailed simulation results data used in Ch.6

Gas	Volume $[m^3]$	$\bar{S}_0$	Vent size 1/16 of the front wall			Vent size 1/8 of the front wall			Vent size 1/4 of the front wall		
			$\bar{A}$	$\bar{A}/\bar{S}_0$	P_m [bar]	$\bar{A}$	$\bar{A}/\bar{S}_0$	P_m[bar]	$\bar{A}$	$\bar{A}/\bar{S}_0$	P_m[bar]
H_2	2	0.044	0.005613	0.1276	5.286	0.012162	0.2764	3.867	0.026351	0.5989	1.937
	4	0.044	0.00625	0.1420	5.128	0.0125	0.2841	3.943	0.025	0.5682	1.916
	20	0.044	0.006722	0.1528	5.063	0.012497	0.2840	3.852	0.024966	0.5674	1.874
	125	0.044	0.00624	0.1418	5.37	0.0125	0.2841	4.13	0.025	0.5682	2.217
CH_4	2	0.0085	0.005613	0.6604	0.84	0.012162	1.4308	0.168	0.026351	3.1002	0.033
	4	0.0085	0.00625	0.7353	0.6	0.0125	1.4706	0.165	0.025	2.9412	0.031
	20	0.0085	0.006722	0.7908	0.4	0.012497	1.4702	0.103	0.024966	2.9371	0.037
	125	0.0085	0.00624	0.7341	0.387	0.0125	1.4706	0.085	0.025	2.9412	0.06
C_2H_4	2	0.014	0.005613	0.4010	3.188	0.012162	0.8687	0.996	0.026351	1.8822	0.163
	4	0.014	0.00625	0.4464	2.628	0.0125	0.8929	0.976	0.025	1.7857	0.163
	20	0.014	0.006722	0.4801	2.168	0.012497	0.8926	0.682	0.024966	1.7833	0.121
	125	0.014	0.00624	0.4457	2.437	0.0125	0.8929	0.654	0.025	1.7857	0.104
C_3H_8	2	0.0099	0.005613	0.5670	1.95	0.012162	1.2285	0.45	0.026351	2.6618	0.08
	4	0.0099	0.00625	0.6313	1.525	0.0125	1.2626	0.45	0.025	2.5253	0.08
	20	0.0099	0.006722	0.6789	1.225	0.012497	1.2623	0.3	0.024966	2.5218	0.063
	125	0.0099	0.00624	0.6303	1.469	0.0125	1.2626	0.3	0.025	2.5253	0.056

Gas	Volume [m³]	$\overline{S}_0$	Vent size 1/2 of the front wall			Vent size 3/4 of the front wall			Vent size 1 of the front wall		
			$\overline{A}$	$\overline{A}/\overline{S}_0$	P_m[bar]	$\overline{A}$	$\overline{A}/\overline{S}_0$	P_m[bar]	$\overline{A}$	$\overline{A}/\overline{S}_0$	P_m[bar]
H_2	2	0.044	0.044906	1.0206	0.93	0.074844	1.7010	0.6	0.097297	2.2113	0.536
	4	0.044	0.051563	1.1719	0.636	0.076563	1.7401	0.5	0.1	2.2727	0.448
	20	0.044	0.05	1.1364	0.596	0.07572	1.7209	0.483	0.1	2.2727	0.468
	125	0.044	0.05	1.1364	0.727	0.07396	1.6809	0.543	0.1	2.2727	0.523
CH_4	2	0.0085	0.044906	5.2831	0.032	0.074844	8.8052	0.026	0.097297	11.4467	0.026
	4	0.0085	0.051563	6.0662	0.026	0.076563	9.0074	0.023	0.1	11.7647	0.023
	20	0.0085	0.05	5.8824	0.033	0.07572	8.9083	0.03	0.1	11.7647	0.031
	125	0.0085	0.05	5.8824	0.039	0.07396	8.7012	0.031	0.1	11.7647	0.025
C_2H_4	2	0.014	0.044906	3.2076	0.051	0.074844	5.3460	0.022	0.097297	6.9498	0.019
	4	0.014	0.051563	3.6830	0.044	0.076563	5.4688	0.021	0.1	7.1429	0.016
	20	0.014	0.05	3.5714	0.102	0.07572	5.4086	0.018	0.1	7.1429	0.023
	125	0.014	0.05	3.5714	0.107	0.07396	5.2829	0.106	0.1	7.1429	0.065
C_3H_8	2	0.0099	0.044906	4.5360	0.046	0.074844	7.5600	0.025	0.097297	9.8280	0.025
	4	0.0099	0.051563	5.2083	0.036	0.076563	7.7336	0.019	0.1	10.1010	0.022
	20	0.0099	0.05	5.0505	0.043	0.07572	7.6485	0.025	0.1	10.1010	0.029
	125	0.0099	0.05	5.0505	0.061	0.07396	7.4707	0.029	0.1	10.1010	0.037

Table 10. Detailed data from comparing results of experiments and simulations used in Ch.6

Reference	Gas	Volume [m³]	$\bar{S}_0$	Gas composition		Vent area		Result	
				Vol %	E_R	$\bar{A}$	$\bar{A}/\bar{S}_0$	EXP_P_m[bar]	SIM_P_m[bar]
Bauwens [2013]	C_3H_8	64	0.0099	4.8	1.2	0.050625	5.1136	0.06	0.09
		64	0.0099	5.2	1.3	0.050625	5.1136	0.07	0.086
		64	0.0099	5.6	1.4	0.050625	5.1136	0.08	0.073
Skjold.T et al., [2017]	H_2	33	0.044	21	0.7	0.035797	0.8136	0.146	0.35
		33	0.044	21	0.7	0.053695	1.2203	0.12	0.248
		33	0.044	21	0.7	0.071594	1.6271	0.19	0.23